Research Article

Leema Rose Ayyasamy, Anbarasu Mohan, Dhanasingh Sivalinga Vijayan*, Agoramoorthy Sattainathan Sharma, Parthiban Devarajan, Aravindan Sivasuriyan

Finite element analysis of behavior and ultimate strength of composite column

https://doi.org/10.1515/secm-2022-0017 received February 18, 2022; accepted June 14, 2022

Abstract: Composite sections are found to be a novel technique in modern day scenario of construction. This stands tall than the ordinary and conventional type of constructions. Columns as a structural element play a vital role in structural frame. This research comments on the behavior of composite columns. The main objective of this study is to analyze the behavior of steelencased concrete composite columns as experimentally under axial compression and the mode of failure under ultimate failure and yield point. The steel-concrete composite system combines the formability and rigidity of reinforced concrete with the ductility and strength of structural steel to meet the demand for earthquake-resistant constructions. Three specimens were chosen for this study: one was a composite column, the other two were ordinary RC columns and structural steel columns. The raw materials' natural properties are assessed. As a result, material testing for cement, fine aggregate, and coarse aggregate was completed, as well as a concrete mix design. A comparative analysis of the local and post-local buckling behavior of different composite sections has been studied and the column sections have been designed according to Eurocode 4 (ENV 1994) to determine the plastic resistance of the section. These three specimens underwent compression test and the results are tabulated and compared. The corrosion resistance and fireproof nature (resistance to fire at

higher temperatures) that are transmitted into the member are related to the steel being encased within the concrete. These are the two major drawbacks of any steel construction combined with an earthquake-resistant structure. Rather than a traditional steel construction, earthquake structures benefit from this type of load handling capabilities. The portion can be used before it completely collapses if proper design factors are taken into account.

Keywords: Ti64, HVOF parameters, SiO coating, POD, Taguchi's technique, GRA, ANOVA

1 Introduction

Composite construction development is inevitable due to its performance, behavior, and its load carrying capacity. Although, the composite construction reduces the time and cost for the medium-rise to high-rise buildings, the usage of different materials in combination yields better results than conventional. In particular, composite beams and slabs are used in the construction places wherever required, since the connections are employed to act together as monolithic. Usually, the composite columns are found either in the form of rolled steel sections embedded in concrete or hollow sections with in filled concrete [1]. Furthermore, the design for evaluating the strength of the components takes into account the composite action in contemporary practice. Since there is no provision for strength, steel column components encased in concrete were used in the fire and corrosion protection of the structural components. In contrast to ordinary joists, rolled steel joists were employed in the column so that the lateral ties offers confining effect in the conventional columns [2-4].

In the composite construction, the plain steel sections usually act as a support to resist the pre-construction loads including with the dead weight of the structure at the stage of construction like a scaffolding. Light weight and high strength could be driven through composite components. Further, it was reported that the steel-encased concrete

Leema Rose Ayyasamy, Agoramoorthy Sattainathan Sharma: Civil Engineering Department, SRM Valliammai Engineering College, Chennai. India

Anbarasu Mohan: Civil Engineering Department, SRM Engineering College, Chennai, India

Parthiban Devarajan, Aravindan Sivasuriyan: Civil Engineering Department, Aarupadai Veedu Institute of Technology, Vinayaka Mission's Research Foundation (VMRF), Chennai, TN, India

^{*} Corresponding author: Dhanasingh Sivalinga Vijayan, Civil Engineering Department, Aarupadai Veedu Institute of Technology, Vinayaka Mission's Research Foundation (VMRF), Chennai, TN, India, e-mail: vijayan@avit.ac.in

composite structural systems increased extensively in the tall building construction and it was also found that the fire resistance of the encased steel tubes with concrete offers is well [5,6]. Marine buildings built with composite materials may be more cost-effective and easier to maintain. Steel stanchions encased in steel reinforcement and concrete are used to protect structural components against fire in steel frame construction [7]. By properly distributing the inducing stresses in the composite column, reducing the column's effective slenderness can increase its buckling load capacity. Figure 1 explains about the application area of composite in the field of civil engineering. In some other study, it was recommended that the composite structural components for the construction of high-rise and medium-rise construction without any justification. Steelencased concrete composite construction does not gain much attention than conventional one due to its construction and design practice [8], and the composite column made of I-shaped thin-walled steel section embedded in concrete [9]. In most of the study, in order to prevent and improve the performance of local buckling the transverse links was used to connect the flanges at regular intervals [10].

Hence, it could be suggested that the implementation of steel-encased concrete composite column for multistorey buildings is proposed to carry the axial and lateral loads developed in the structural systems which were resisted by shear walls. Composite construction offers much on ductility, strength, and stiffness of the structural components. Steel tube with infilled concrete avoids the formwork and causes reduction in construction time automatically [11]. The confinement effect also boosts

the load carrying capability of the infilled concrete tubes. Confinement efficiency is determined by the shape of the steel tube and column, structural steel yield strength, and concrete's characteristic compressive strength [8]. Addition of steel plates in the composite structures made of steel sections infilled with concrete is increased tremendously under seismic action due to its high stiffness, energy absorption capacity and strength, and ductility. Mirza et al. found that the addition of steel plate as confinement in composite component enhances the ductility in which the inward buckling is observed in the steel plate may leads high impact resistance. Hot rolled steel sections with concrete is advisable in the composite construction. No formwork could be required in the composite construction with efficient time management [12,13] and the properties were investigated using finite element analyses on composite column [14-16].

Indian standard medium beam (ISMB) 100 is inserted into concrete with a circular section in this study to properly transmit the load with higher load carrying capability and to advise design practices from various codes. The effectiveness of the composite effect will also be evaluated in comparison to traditional reinforced concrete and steel columns.

2 Experimental investigation

Concrete mix in the proportion of 1:1.6:2.56 is used and designed using IS 10262 (2009) in which water-cement ratio is 0.45. Cement (OPC 53) and aggregates confirming

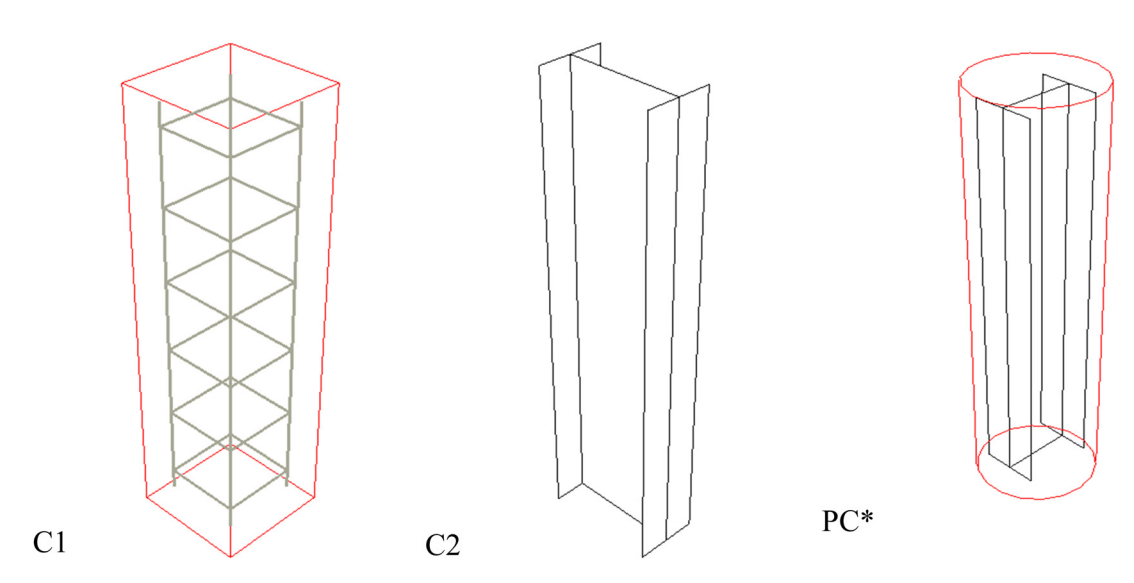


Figure 1: Geometrical configurations in modeling.

Indian Standards IS 4031-6 (1988) and IS 2386 (1963), respectively, are shown in Table 1. The characteristic compressive and split tensile strength at 28 days are 32.8 and 3.18 MPa. Specimen details of the experiment are given in Table 2 and are subjected to axial compression.

Both ISMB sections and reinforcement yield stress (f_y) are 250 and 415 MPa, respectively. The characteristic compressive strength of concrete $(f_{\rm ck})$ is 30 MPa. Concrete effective cover is 25 mm. Strain gauges were located at the middle of the specimen along the length.

3 Analytical studies

Designs of the columns PC*, C1, and C2 were carried out by confirming Eurocode 4 (1994), IS 456 (2000), and IS 800 (2007), respectively [17].

Case 1 - Conventional RCC column (C1):

Factored axial load of the RC column is as follows:

$$P_{\rm u} = 0.4 f_{\rm ck} A_{\rm c} + 0.67 f_{\rm v} A_{\rm sc}.$$
 (1)

Area of concrete (A_c) and steel (A_{sc}) are 22,500 and 314.15 mm², respectively.

Length (l), breadth (B), and depth (D) of the column are 600, 150, and 150 mm, respectively. Four numbers of longitudinal reinforcement (dia. 10 mm) are provided.

$$\frac{l_e}{D}$$
 = 4 < 12, (Short column, IS 456).

Case 2 - Conventional steel column (C2):

Factored axial load of steel column (ISMB 150) is as follows:

$$P_{\rm d} = A_{\rm c} F_{\rm cd}. \tag{2}$$

Length (l), area ($A_{\rm e}$), non-dimensional parameter (λ), ϕ , reduction factor (χ), and $F_{\rm cd}$ are 600 mm, 1,900 mm², 0.406, 0.617, 0.92, and 170 MPa, respectively (IS 800).

Case 3 – Proposed composite column (PC*):

Plastic resistance of composite column is as follows:

$$P_{\rm p} = \frac{A_{\rm a} f_{\rm y}}{Y_{\rm a}} + \frac{0.85 A_{\rm c} f_{\rm ck}}{Y_{\rm c}}.$$
 (3)

Area and partial safety factors in equation (1) are presented in Table 3.

4 Numerical analysis

Finite element analysis (FEA) is carried out on the specimens given in Table 4 under axial compression using commercial FE tool (Abagus), Concrete damaged plasticity model is used for the concrete, since steel follows the bi-linear stress-strain curve. Bottom of the specimen is pinned, since it is in practice during experimentation. For convergence of the solution to appropriate conclusions, the physical domain under inquiry is subjected to limitations, called boundary conditions, in FEA. In FEA, symmetric boundary conditions are constraints that reduce the amount of computer memory and simulation time used. Steel and concrete properties were taken, respectively [18,19]. Newton-Raphson method is used in the numerical increments. ISMB sections were modelled using shell elements, and the shell element analysis produced solid elements that were very close approximations. Hence, employing shell elements instead of solid elements could reduce much on computational cost. Reinforcement and ISMB 100 were embedded in concrete to simulate the effect of composite in C1 and C2, respectively. Element size is fixed based on the mesh sensitivity analysis and experimental results [20]. Figure 1 depicts the geometrical configuration of composite modeling. Element size of concrete, ISMB sections, and reinforcement is 20 mm for all C1, C2, and PC*. Eight noded solid element with reduced integration, four noded shell element with reduced integration, and two noded beam element are employed for concrete, ISMB sections, and reinforcement, respectively.

Table 1: Properties of materials

Test	Cement	Fine aggregate	Coarse aggregate
Consistency, (%)	33	_	_
Initial setting time, (min)	42	_	_
Final setting time, (min)	275	_	_
Specific gravity	3.15	2.6	2.65
Fineness	2.9	3.07	7.3

Table 2: Experimental details

Specimen ID	Depth (mm)	Width (mm)	Thickness (mm)		Remarks
			Flange	Web	
C1	150	150	_	_	Conventional RC** column, 4# 10 mm dia.
C2	150	80	7.6	4.8	Conventional steel column, ISMB 150
PC [*]	100	75	7.2	4.0	$\operatorname{Column}-\operatorname{ISMB}$ 100 encased with concrete

^{*} Proposed composite column; **Reinforced concrete.

Table 3: Area and partial safety factors of materials

Properties	Structural steel	Concrete
Partial safety factor Area (mm²)	$\gamma_a = 1.10$ $A_a = 1460$	$\gamma_{c} = 1.5$ $A_{c} = 16211.46$

Table 4: Ultimate load carrying capacity of specimens

Specimen ID	Ultimate load (kN)			
	Experimental	Analytical	Numerical	
PC*	637.6	607.46	577.41	
C1	471.8	353.57	498.06	
C2	428.2	323	515.91	

^{*} Proposed composite column.

5 Results and discussion

Factored axial load of PC*, C1, and C2 are 607.46, 498.06, and 515.91, respectively. It can be clearly noted that the factored axial load of PC* is increased by 71.8 and 88.1% with respect to C1 and C2, respectively. From Table 4, it

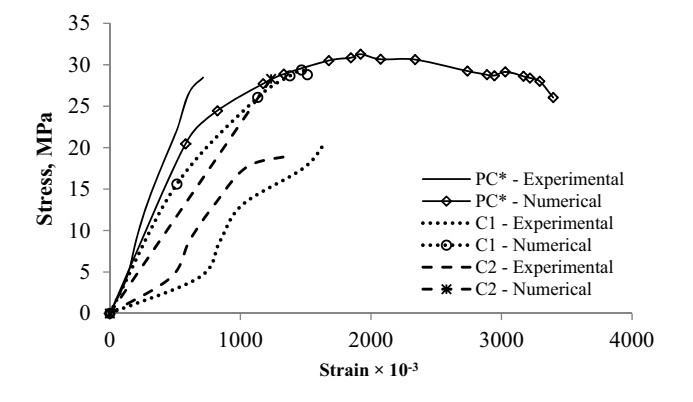


Figure 2: Stress-strain behavior.

can be observed that the increase load carrying capacity of PC is 16 and 12, and 35 and 48.9 % for C1 and C2, respectively, with respect to numerical and experimental. So, the composite effect can be found from analytical equation itself and the same is reflected in the experimentation and FEA. Ultimate load of the specimens are tabulated in Table 4. So, the proposed composite column (PC*) is exhibiting the higher load carrying capacity than others. Table 4 details the ultimate load carrying capacity of the specimens investigated.

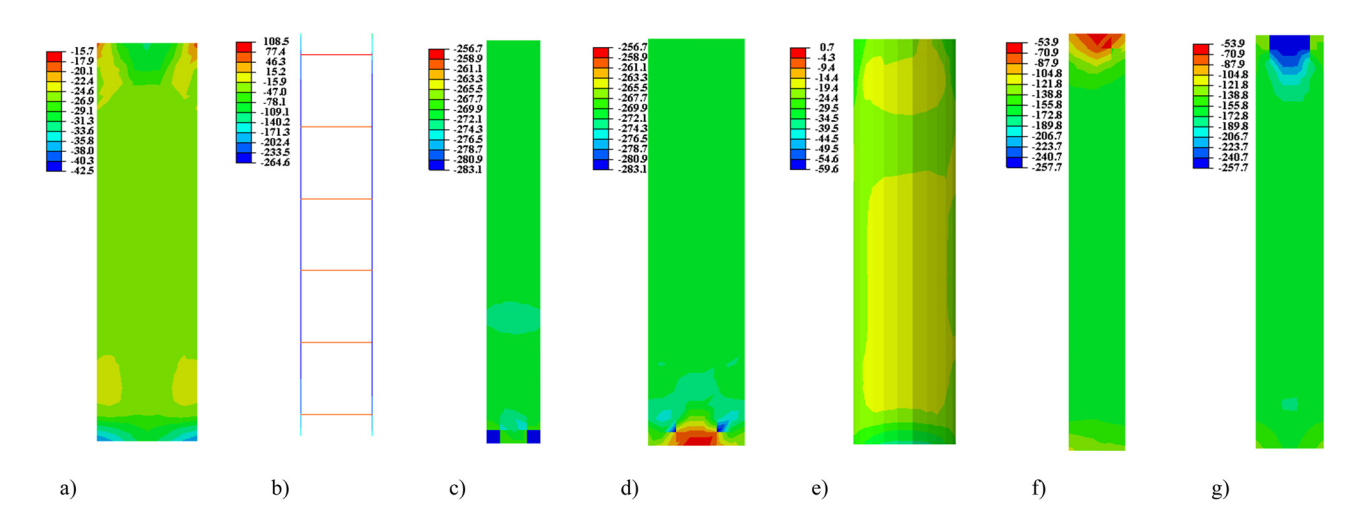


Figure 3: Stress distribution at peak load: (a) C1-Concrete, (b) C1-Rebar, (c) C2-Web, (d) C2-Flange, (e) PC-Concrete, (f) PC-Web, and (g) PC-Flange.

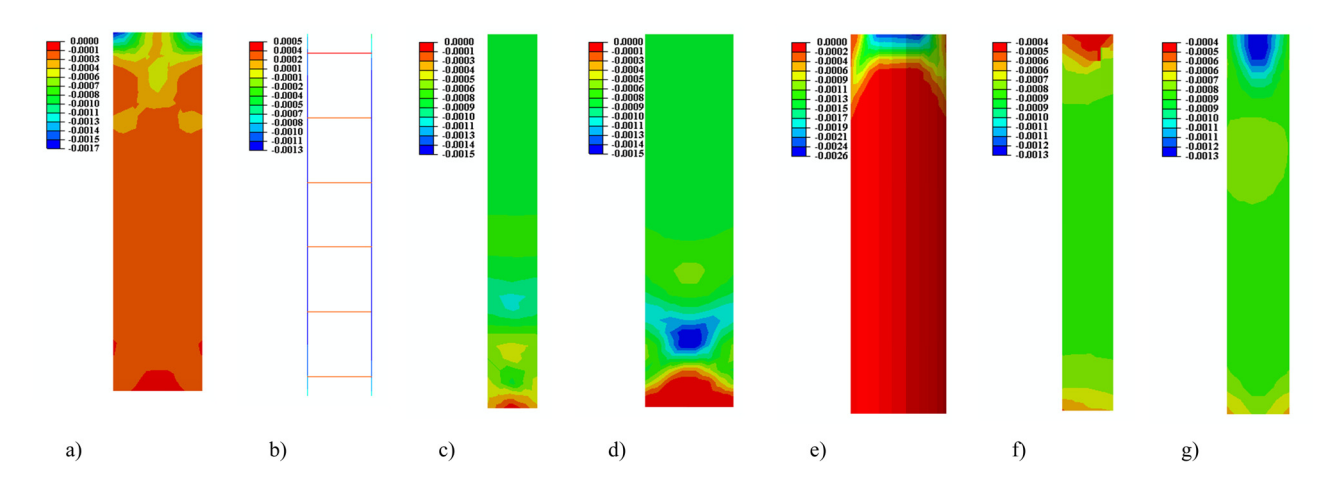


Figure 4: Strain distribution at peak load: (a) C1-Concrete, (b) C1-Rebar, (c) C2-Web, (d) C2-Flange, (e) PC-Concrete, (f) PC-Web, and (g) PC-Flange.

The stress–strain behavior of the specimens is exhibited in Figure 2. FEA resulted in good agreement with the experimentation. From Figure 2, it can be noted that experimentally measured stress values of C1, C2, and PC are 20.71 19.1, and 28.45 MPa, respectively, whereas the characteristic compressive strength of concrete is 32.8 MPa. Also, it can be clearly noted that the numerically obtained stress values of C1, C2, and PC are 28.3, 28.66, and 31.28 MPa, respectively from Figure 2. The ultimate strain difference (at peak stress) between the experimentation and numerical

is very minimal. Especially, the obtained numerical result is in better agreement with the experimental result. So, the numerical models constructed were well suited and could be used to capture other physical quantities.

Figure 3a–g exhibits the stress distribution at peak load for C1-Concrete, C1-Rebar, C2-Web, C2-Flange, PC-Concrete, PC-Web, and PC-Flange, respectively [21]. Stress reaches around 30 MPa in concrete for C1 and PC specimens in Figure 3a–e. Observed maximum stress in reinforcement (C1), ISMB 150 (C2), and ISMB 100 (PC) is 264.6, 283.1 and

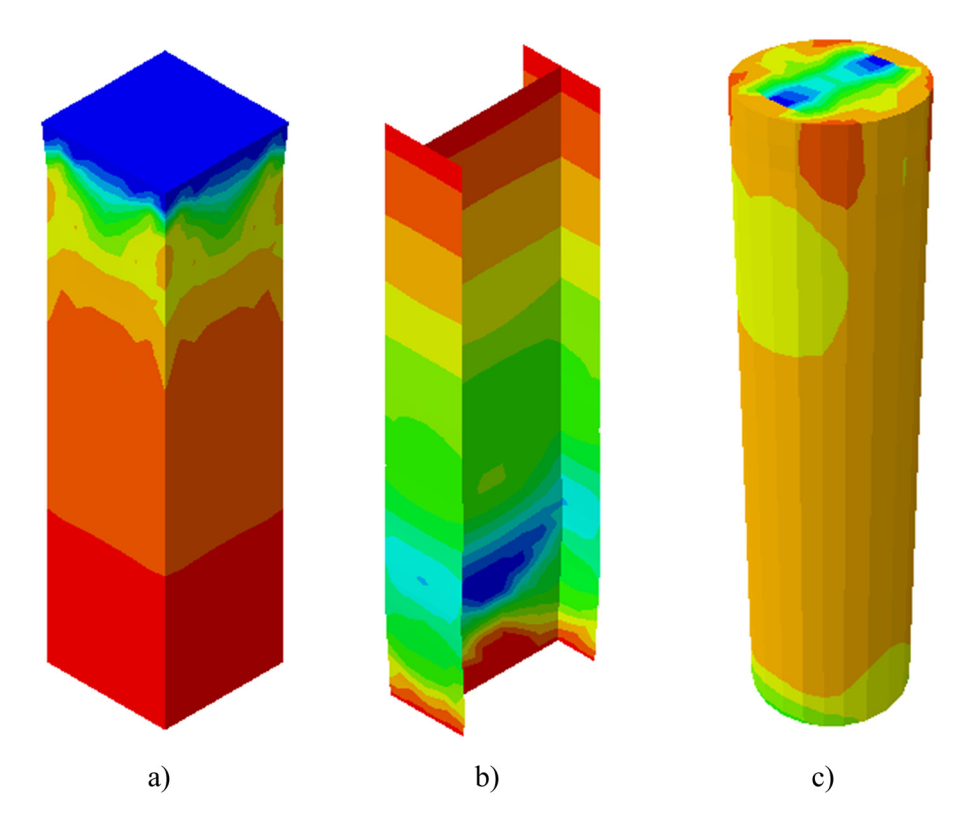


Figure 5: Final failure profile: (a) C1, (b) C2, and (c) PC.

257.7 MPa, respectively. Stress in PC varies from 8 to 25 MPa lesser than C1 and C2, respectively, due to the development of composite effect and the geometrical effect [22].

Figure 4a-g exhibits the strain distribution at peak load along the length of the specimens C1-Concrete, C1-Rebar, C2-Web, C2-Flange, PC-Concrete, PC-Web, and PC-Flange, respectively. Strains in concrete and reinforcement are 0.0017 and 0.0013, respectively, since the maximum load reaches lateral tie confinement before yielding strain in concrete of 0.002. Strains in ISMB 150 and 100 are 0.0015 and 0.0013, respectively, whereas the change in strain is in negligible amount. It reveals that the maximum usage of ISMB 100 in the PC is due to composite effect. At the same time, the maximum strain of 0.0026 is observed in PC-Concrete. So, the yielding point beyond 0.0026 is found to be achieved due to the compatibility between the ISMB 100 section and concrete and leads to better composite effect with almost no confinement [23]. Figure 5 shows the final failure profile of the specimens.

6 Conclusion

Experiments have been carried out on conventional RC column, conventional steel column, and the composite column to increase the ultimate load carrying capacity in which the composite column is the proposed one. Analytical evaluations on load carrying capacity based on the codes IS 456, IS 800, and Eurocode 4 were carried out. The composite column is found to be a better load carrying specimen PC than the other from the analytical solution which itself reveals the high load carrying capacity due to the composite effect and the same is resulted from experiment and FEA. It can concluded that the increase in load carrying capacity of the proposed section is quite high than the conventional concrete and steel columns. Also, from the FEA results, the stress and strain distribution along the length exhibits the pattern in practice and the observed values also indicate the composite effect of the proposed column in good manner.

Acknowledgments: Research outcomes of the manuscript was supported by Aarupadai Veedu Institute of Technology, Chennai. We would also like to extend our thanks to the authors for providing the technical support needed.

Funding information: This research did not receive any specific grant from funding agencies in the public, commercial, or not-for-profit sectors.

Author contributions: Leema Rose Ayyasamy: validation, editing, reviewing, and supervision; A. Mohan and Dhanasingh Sivalinga Vijayan: collecting research data, writing - original draft, methodology, and modeling in abacus; Agoramoorthy Sattainathan Sharma: experimental work, grammar, and English correction; Parthiban Devarajan: modeling and rewriting; Aravind Sivasuriyan: experimental work and data acquisition.

Conflict of interest: The authors declare that they have no known competing financial interests or personal relationships that could have appeared to influence the work reported in this article.

Consent to participate: No human subjects or animals are used for the research in the manuscript. Hence there no consent to participate required.

Consent to publish: No human subjects or animals are used for the research in the manuscript. Hence there no consent to publish required.

Ethical approval section: Not applicable.

Data availability statement: The authors declare that (the/all other) data supporting the findings of this study are available within the article and its supplementary information files.

References

- [1] Chen SF, Teng JG, Chan SL. Design of biaxially loaded short composite columns of arbitrary section. J Struct Eng. 2001 Jun;127(6):678-85.
- Weng CC, Yen SI. Comparisons of concrete-encased composite [2] column strength provisions of ACI code and AISC specification. Eng Struct. 2002;24(1):59-72.
- [3] Ellobody E, Young B, Lam D. Behaviour of normal and high strength concrete-filled compact steel tube circular stub columns. J Constr Steel Res. 2006;62(7):706-15.
- [4] Chen CC, Lin NJ. Analytical model for predicting axial capacity and behavior of concrete encased steel composite stub columns. J Constr Steel Res. 2006;62(5):424-33.
- Chicoine T, Massicotte B, Tremblay R. Long-term behavior and strength of partially encased composite columns made with built-up steel shapes. J Struct Eng. 2003;129(2):141-50.
- El-Tawil S, Deierlein GG. Strength and ductility of concrete [6] encased composite columns. J Struct Eng [Internet]. 1999 Sep;125(9):1009-19.
- [7] Vijayan DS, Revathy J. Experimental investigation on the static performance of GFRP strengthened prestressed concrete beams. World Appl Sci J. 2016;34(10):1366-9.

- [8] Mursi M, Uy B. Strength of concrete filled steel box columns incorporating interaction buckling. J Struct Eng. 2003;129(5):626–39.
- [9] Wright HD. Local stability of filled and encased steel sections.J Struct Eng. 1995 Oct;121(10):1382-8.
- [10] Kim C-S, Park H-G, Chung K-S, Choi I-R. Eccentric axial load capacity of high-strength steel-concrete composite columns of various sectional shapes. J Struct Eng. 2014;140(4):04013091.
- [11] Dundar C, Tokgoz S, Tanrikulu AK, Baran T. Behaviour of reinforced and concrete-encased composite columns subjected to biaxial bending and axial load. Build Environ. 2008;43(6):1109–20.
- [12] Mirza SA, Lacroix EA. Comparative strength analyses of concrete-encased steel composite columns. J Struct Eng. 2004 Dec:130(12):1941-53.
- [13] Lee J, Nguyen HT, Kim S-E. Buckling and post buckling of thinwalled composite columns with intermediate-stiffened open cross-section under axial compression. Int J Steel Struct. 2009;9(3):175-84.
- [14] Vijayan DS, Revathy DJ. Flexural behavior of reinforced and pre-stressed concrete beam using finite element method. Int J Appl Eng Res. 2015;10. doi: 10.17485/ijst/2016/v9i42/101824. http://www.ripublication.com.
- [15] Mehrabani R, Shanmugam NE. Finite element analysis of the behaviour and ultimate strength of battened columns encased in concrete. IES J Part A Civ Struct Eng. 2014;7(4):263–80.

- [16] Yonas TY, Temesgen W, Senshaw FW. Finite element analysis of slender composite column subjected to eccentric loading. Int J Appl Eng Res. 2018;13(15):11730-7.
- [17] IS 456. Plain concrete and reinforced. New Delhi: Bureau of Indian Standards; 2000. p. 1–114.
- [18] Dar MA, Subramanian N, Dar AR, Anbarasu M, Lim JBP, Atif M. Behaviour of partly stiffened cold-formed steel built-up beams: experimental investigation and numerical validation. Adv Struct Eng. 2019;22(1):172–86.
- [19] Hafezolghorani M, Hejazi F, Vaghei R, Jaafar MSB, Karimzade K. Simplified damage plasticity model for concrete. Struct Eng Int. 2017;27(1):68–78.
- [20] Parthiban D, Vijayan DS. Study on stress-strain effect of reinforced metakaolin based GPC under compression. Mater Today: Proc; 2020. p. 822-8. doi: 10.1016/ j.matpr.2019.10.162.
- [21] Vaverková MD, Radziemska M, Bartoň S, Cerdà A, Koda E. The use of vegetation as a natural strategy for landfill restoration. Land Degrad Dev. 2018;29(10):3674–80.
- [22] Koda E, Kiersnowska A, Kawalec J, Osiński P. Landfill slope stability improvement incorporating reinforcements in reclamation process applying observational method. Appl Sci. 2020;10(5). doi: 10.3390/app10051572.
- [23] IS 456. Plain and reinforced concrete code of practice. New Delhi: Bureau of Indian Standards; 2000. p. 1–114.